

 Open access • Journal Article • DOI:10.1063/1.3334729

Role of field-effect on c-Si surface passivation by ultrathin (2–20 nm) atomic layer deposited Al₂O₃ — [Source link](#)

NM Nick Terlinden, G Gijs Dingemans, van de Mcm Richard Sanden, Wmm Erwin Kessels

Published on: 15 Mar 2010 - Applied Physics Letters (American Institute of Physics)

Topics: Passivation, Atomic layer deposition, Chemical vapor deposition, Layer (electronics) and Crystalline silicon

Related papers:

- [Ultralow surface recombination of c-Si substrates passivated by plasma-assisted atomic layer deposited Al₂O₃](#)
- [On the c-Si surface passivation mechanism by the negative-charge-dielectric Al₂O₃](#)
- [Very low surface recombination velocities on p-type silicon wafers passivated with a dielectric with fixed negative charge](#)
- [Silicon surface passivation by atomic layer deposited Al₂O₃](#)
- [Silicon surface passivation by ultrathin Al₂O₃ films synthesized by thermal and plasma atomic layer deposition](#)

Share this paper:    

View more about this paper here: <https://typeset.io/papers/role-of-field-effect-on-c-si-surface-passivation-by-36kb6x6gcb>

Role of field-effect on c-Si surface passivation by ultrathin (2-20 nm) atomic layer deposited Al₂O₃

Citation for published version (APA):

Terlinden, N. M., Dingemans, G., Sanden, van de, M. C. M., & Kessels, W. M. M. (2010). Role of field-effect on c-Si surface passivation by ultrathin (2-20 nm) atomic layer deposited Al₂O₃. *Applied Physics Letters*, 96(11), 112101-1/3. [112101]. <https://doi.org/10.1063/1.3334729>

DOI:

[10.1063/1.3334729](https://doi.org/10.1063/1.3334729)

Document status and date:

Published: 01/01/2010

Document Version:

Publisher's PDF, also known as Version of Record (includes final page, issue and volume numbers)

Please check the document version of this publication:

- A submitted manuscript is the version of the article upon submission and before peer-review. There can be important differences between the submitted version and the official published version of record. People interested in the research are advised to contact the author for the final version of the publication, or visit the DOI to the publisher's website.
- The final author version and the galley proof are versions of the publication after peer review.
- The final published version features the final layout of the paper including the volume, issue and page numbers.

[Link to publication](#)

General rights

Copyright and moral rights for the publications made accessible in the public portal are retained by the authors and/or other copyright owners and it is a condition of accessing publications that users recognise and abide by the legal requirements associated with these rights.

- Users may download and print one copy of any publication from the public portal for the purpose of private study or research.
- You may not further distribute the material or use it for any profit-making activity or commercial gain
- You may freely distribute the URL identifying the publication in the public portal.

If the publication is distributed under the terms of Article 25fa of the Dutch Copyright Act, indicated by the "Taverne" license above, please follow below link for the End User Agreement:

www.tue.nl/taverne

Take down policy

If you believe that this document breaches copyright please contact us at:

openaccess@tue.nl

providing details and we will investigate your claim.

Role of field-effect on *c*-Si surface passivation by ultrathin (2–20 nm) atomic layer deposited Al₂O₃

N. M. Terlinden,^{a)} G. Dingemans, M. C. M van de Sanden, and W. M. M. Kessels^{a)}

Department of Applied Physics, Eindhoven University of Technology, P.O. Box 513, 5600 MB Eindhoven, The Netherlands

(Received 12 January 2010; accepted 4 February 2010; published online 15 March 2010)

Al₂O₃ synthesized by plasma-assisted atomic layer deposition yields excellent surface passivation of crystalline silicon (*c*-Si) for films down to ~5 nm in thickness. Optical second-harmonic generation was employed to distinguish between the influence of field-effect passivation and chemical passivation through the measurement of the electric field in the *c*-Si space-charge region. It is demonstrated that this electric field—and hence the *negative* fixed charge density—is virtually unaffected by the Al₂O₃ thickness between 2 and 20 nm indicating that a decrease in chemical passivation causes the reduced passivation performance for <5 nm thick Al₂O₃ films. © 2010 American Institute of Physics. [doi:10.1063/1.3334729]

The reduction in surface recombination losses is of prime importance for next generation crystalline silicon (*c*-Si) solar cells, as the interface characteristics play a vital role in the overall solar cell performance. Surface passivation can be obtained either by reducing the interface defect density, i.e., chemical passivation, or by shielding the minority carriers from the semiconductor interface by means of a built-in electric field, i.e., field-effect passivation.¹ Such passivation mechanisms can be induced by applying functional thin films to the surface of *c*-Si. It has been shown that amorphous Al₂O₃ thin films synthesized by (plasma-assisted) atomic layer deposition (ALD) provide excellent surface passivation of *n*, *p*, and *p*⁺-type *c*-Si.^{2–4} In addition to the chemical passivation, a strong field-effect passivation was found to play a key role in the passivation mechanism of Al₂O₃, due to the presence of a high *negative* fixed charge density in Al₂O₃.^{1,5}

Recently, it was demonstrated that Al₂O₃ films synthesized by plasma-assisted ALD yield an excellent, constant level of surface passivation of *c*-Si for films down to ~5 nm thickness, but deteriorates significantly for film thicknesses below this typical value.⁶ Whether this deterioration is related to a decrease in the chemical or field-effect passivation, or both, has not yet been elucidated. Therefore, in this letter, we further investigate the influence of Al₂O₃ film thickness on the *c*-Si surface passivation quality, as the film thickness is a critical parameter considering the ALD processing speed. We employ the nonlinear optical technique of second-harmonic generation (SHG), which is contactless, noninvasive, and has intrinsically no requirement on minimum film thickness, unlike more conventional techniques. Moreover, SHG is sensitive to internal electric fields (>10⁵ V·cm⁻¹) in silicon/thin film systems through the effect of electric-field-induced SHG (EFISH) and can be used to investigate field-effect passivation. We demonstrate that the field-effect passivation is virtually unaffected by the Al₂O₃ film thickness down to 2 nm, which indicates that a decrease in chemical passivation causes the reduced surface passivation performance for <5 nm thick films.

Ultrathin films of Al₂O₃ with a thickness of 2–20 nm were deposited at both sides of *p*-type (275 μm, <100>, ~2 Ω·cm) float zone *c*-Si wafers preceded by a HF dip to remove the native oxide. The films were synthesized by plasma-assisted ALD at a substrate temperature of 200 °C, yielding films with an O/Al ratio of 1.5–1.6, negligible carbon content (<2 at. %), and a small amount of hydrogen (~2–3 at. %).⁷ Previously, also the presence of an interfacial SiO_x layer (1.2–1.5 nm) between the Si wafer and the Al₂O₃ was observed by high-resolution transmission electron microscopy.³ After deposition, the samples received a post-deposition anneal (PDA) for 10 min at 400 °C in N₂, necessary to activate the passivation.^{3,4} To provide a measure for the level of field-effect passivation, the electric field in the *c*-Si space-charge region (SCR), as caused by the *negative* fixed charge in Al₂O₃, has been probed using SHG. Being surface and interface specific for isotropic media and resonant with optical transitions, SHG allows for the contactless probing of the properties of the interface between thin films and the *c*-Si substrate. SHG measurements were performed using *p*-polarized femtosecond (~90 fs) laser radiation from a Ti:sapphire oscillator, tunable in the 1.33–1.75 eV photon energy range, and focused on the sample at a 35° angle of incidence to a spot size of ~100 μm. SHG radiation generated in reflection, using a fluence at the sample of ~4 μJ·cm⁻² per pulse, was separated from the fundamental radiation using optical and spatial filtering and detected in *p*-polarization with a photomultiplier tube connected to single photon counting electronics.⁸ In addition, the surface passivation quality, depending on both chemical and field-effect passivation, is given in terms of the upper limit of the effective surface recombination velocity $S_{eff,max}$. Its value is calculated from the effective lifetime (τ_{eff}) of the minority carriers at an injection level of 10¹⁵ cm⁻³, assuming an infinite bulk lifetime. The τ_{eff} values were obtained by contactless photoconductance decay measurements performed in transient mode.

In Fig. 1(a) the obtained $S_{eff,max}$ values are shown as a function of Al₂O₃ film thickness. A virtually constant, high level of surface passivation is obtained for films down to ~5 nm thickness corresponding to values of $S_{eff,max} \leq 23$ cm/s. For thinner films the passivation quality reduces

^{a)}Electronic addresses: n.m.terlinden@tue.nl and w.m.m.kessels@tue.nl.

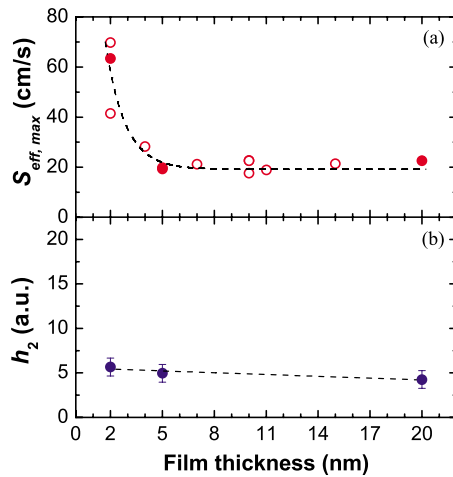


FIG. 1. (Color online) (a) The effective surface recombination velocity $S_{eff,max}$ for ~ 2 Ω -cm p -type Si(100) passivated on both sides with plasma-assisted ALD Al_2O_3 as a function of film thickness. (b) EFISH amplitude h_2 for the Al_2O_3 films corresponding to the solid data markers in (a). The lines serve as a guide to the eye.

significantly as indicated by the increase in $S_{eff,max}$. In comparison, the lowest $S_{eff,max}$ value reported to date is ~ 0.8 cm/s for plasma-assisted ALD Al_2O_3 on 3.5 Ω -cm n -type c -Si.⁶ Most probably, the bulk lifetime of the Si wafers used in this study limits the level of surface passivation that can be observed, as the lifetime depends on wafer type, quality, and doping level. Because $S_{eff,max}$ is ruled by both passivation mechanisms, it is not clear whether the trend in Fig. 1(a) can be attributed to changes in chemical or field-effect passivation.

To investigate the influence of the film thickness on the level of field-effect passivation, spectroscopic SHG measurements were performed for 2, 5, and 20 nm thick films. In Fig. 2 the SHG spectra are shown in the $2\hbar\omega = 2.6$ – 3.6 eV SHG photon energy range. The distinct resonance in all spectra at a SHG photon energy of ~ 3.4 eV corresponds to Si interband transitions at the E'_0/E_1 critical point (CP). For increasing film thickness a slight decrease in the overall SHG intensity can be observed together with a minor blue shift of the resonance peak. A good reproducibility of the SHG measure-

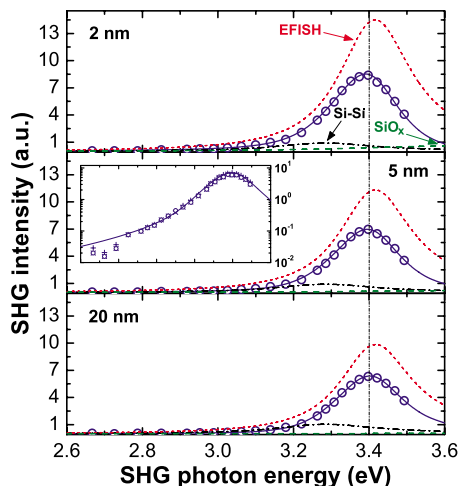


FIG. 2. (Color online) SHG spectra for Al_2O_3 films with a thickness of 2, 5, and 20 nm on Si(100). The solid lines are fits to the data using a superposition of three CP-like resonances as represented by the dashed lines. The inset shows SHG spectra of the 5 nm film for three independent measurements plotted at logarithmic scale.

TABLE I. Parameters of the three CP resonances as obtained from the fits to the SHG spectra in Fig. 2. In the analysis φ_1 is set to zero. Parameter values in italic had a single fit parameter in the multisample fitting procedure and parameter values in bold were fixed.

	2 nm	5 nm	20 nm
Si-Si interface resonance			
h_1 (a.u.)	2.04	2.04	2.04
$\hbar\omega_1$ (eV)	3.27	3.27	3.27
$\hbar\Gamma_1$ (eV)	0.16	0.16	0.16
EFISH resonance			
h_2 (a.u.)	5.66	4.96	4.26
$\hbar\omega_2$ (eV)	3.412	3.412	3.412
$\hbar\Gamma_2$ (eV)	0.117	0.117	0.117
φ_2 (π rad)	0.98	0.98	0.98
SiO _x interface resonance			
h_3 (a.u.)	3.34	1.94	0.69
$\hbar\omega_3$ (eV)	3.62	3.62	3.62
$\hbar\Gamma_3$ (eV)	0.36	0.36	0.36
φ_3 (π rad)	0.33	0.33	0.33

ments is illustrated by the inset of Fig. 2, showing SHG spectra of the 5 nm film for three independent measurements at logarithmic scale. The spectra for the 2 and 20 nm films exhibit the same reproducibility (not shown). Previously, it has been shown that multiple resonances contribute to the SHG response of Al_2O_3 , including the aforementioned electric-field induced contribution.⁵ To separate the different contributions, the spectra have been reproduced using a model in which the SHG intensity is approximated by a coherent superposition of CP-like resonances with excitonic line shapes evaluated at the substrate/film interface^{8–10}

$$I(2\omega) \propto \left| A_{zzz}(\omega, \theta) \sum_q \frac{h_q e^{i\varphi_q}}{2\omega - \omega_q + i\Gamma_q} \right|^2 I_{in}^2(\omega), \quad (1)$$

where I_{in} is the intensity of the incident fundamental radiation. In this equation h_q denotes the (real) amplitude, ω_q the frequency, Γ_q the linewidth, and φ_q the excitonic phase of resonance q . The complex function $A_{zzz}(\omega, \theta)$ in Eq. (1) describes the propagation of both the fundamental and SHG radiation through the thin film system and includes linear optical phenomena, such as absorption, refraction, and interference due to multiple reflections. The required optical constants and film thicknesses were determined by spectroscopic ellipsometry.

Following the approach of Rumpel *et al.*¹¹ for c -Si/SiO_x, three distinct resonances are used in the model to fit the experimental data, which has proven to also be viable for the c -Si/ Al_2O_3 system.⁵ It must be stressed at this point that within the fundamental photon energy range available, SHG originates *only* from transitions in Si at the interface with the film. To obtain a stable and unique fit, as few as possible independent fit parameters were used and the modeling was done simultaneously for all three spectra. The parameters resulting from this analysis are listed in Table I. Note that the separate contributions shown in Fig. 2 are summed taking their phase differences into account [cf. Eq. (1)]. The data in Fig. 2 for the 2, 5, and 20 nm Al_2O_3 can be fitted very well, corresponding to a reduced chi-squared value of 2.9, with a main contribution at 3.41 eV and additional contributions at 3.27 and 3.62 eV. The resonance frequency, linewidth, and phase of the latter have been fixed, as within the current experimental photon energy range the parameters of this contribution cannot be determined unambiguously, and their val-

ues were taken from literature.¹¹ The contribution at 3.27 eV can be assigned to interband transitions related to Si–Si bonds modified due to the vicinity of the interface with the film.^{12,13} This contribution has only minor impact and is constant for all three spectra. The resonance at 3.62 eV originates from strongly distorted Si bonds in a thin transition layer between Si and the interfacial SiO_x.^{11,14} The most dominant contribution at 3.41 eV is a clear signature of EFISH originating from the bulk SCR in *c*-Si. The obtained energy and linewidth for this resonance are very close to the values for bulk Si (3.40 and 0.10 eV, respectively⁹). Note that in general, EFISH is a third-order nonlinear process, described by a rank-four susceptibility tensor, while the other contributions are second-order. However, with a dc electric field perpendicular to the interface, symmetry considerations allow EFISH to be described as a second-order effect.⁸ As shown in Table I both the EFISH amplitude h_2 and the amplitude h_3 of the SiO_x interface resonance decrease for increasing film thickness. Together this causes the slight decrease in SHG intensity and minor blue shift in the peak energy (Fig. 2) as a result of the coherent superposition of the two resonances.

As previously shown, a strong electric field is created at the interface by the large fixed *negative* charge density in the Al₂O₃.⁵ Indeed, the phase difference between the Si–Si interface resonance and the EFISH contribution of $\sim\pi$ (Table I) indicates a *positively* charged SCR in the Si.¹¹ The amplitude of the EFISH contribution is proportional to the magnitude of the electric field in the Si SCR. As this electric field is responsible for the induced field-effect passivation, the EFISH amplitude can be used as a measure for the level of field-effect passivation. In Fig. 1(b) the EFISH amplitude h_2 is plotted as a function of Al₂O₃ film thickness. Within the error, estimated from the accuracy of the experiments and the modeling, h_2 is independent of the film thickness. This means that the magnitude of the electric field in the silicon SCR, and hence the negative fixed charge density (10^{12} – 10^{13} cm⁻²) present in the Al₂O₃, is virtually constant with film thickness. The h_2 values found are indicative of a typical electric field of ~ 170 kV·cm⁻¹ at the Si/SiO_x interface. As this electric field is responsible for the field-effect passivation, a constant magnitude implies that also the field-effect passivation is independent of film thickness. Moreover, it also implies that the charge is located at the SiO_x/Al₂O₃ interface. This is in good agreement with conventional *C-V* measurements that we performed for TiN/Al₂O₃ capacitor stacks on *p*-type *c*-Si, where the films were deposited by plasma-assisted ALD at 400 °C in a similar reactor as used for this study.¹⁵ These measurements showed a linear dependence of the flatband voltage V_{fb} with Al₂O₃ film thickness (10–30 nm). This result also suggests that the fixed charge [$(9.6 \pm 0.2) \times 10^{12}$ cm⁻²] is located near the *c*-Si/Al₂O₃ interface, corresponding to what has been reported by other authors.^{16,17}

From the fact that the field-effect passivation is independent of the film thickness, it can be concluded that the reduced surface passivation quality for <5 nm films [Fig. 1(a)] is caused by a decrease in the level of chemical passivation. As the chemical passivation is related to the defect density at the Si interface, a plausible hypothesis for a decrease in chemical passivation is related to the hydrogen present in Al₂O₃. Hydrogen, available via diffusion from the

Al₂O₃ bulk, is expected to provide chemical passivation by eliminating dangling bonds at the Si interface. Therefore, when the Al₂O₃ film thickness decreases, the amount of hydrogen available for chemical passivation will decrease and/or the hydrogen will become less effective in passivating the surface defect states. This will reduce the surface passivation quality despite of the remaining high level of field-effect passivation. The influence of other interfacial effects (e.g., stress-induced) can however also not be excluded. Considering the change in amplitude h_3 with thickness (Table I), investigations of the SiO_x interface resonance could be a good starting point for further research into the chemical passivation properties.

In conclusion, we have shown that the field-effect passivation of *c*-Si is virtually unaffected by the Al₂O₃ film thickness down to 2 nm, which indicates that a decrease in chemical passivation causes the reduced passivation performance for <5 nm thick films. Moreover, the results demonstrate that SHG allows for the contactless characterization of electric fields in (ultra)thin film systems, which is not feasible by conventional techniques such as *C-V* measurements and corona charging. Being all-optical, SHG is also applicable *in situ* and real-time during processing of passivating thin films (Al₂O₃, *a*-SiN_x:H, *a*-Si:H, and SiO_x) as has recently been demonstrated for *a*-Si:H.^{18,19}

The authors thank P.M. Gevers and Dr. J. J. H. Gielis for their contribution. This work was supported by the Netherlands Organisation for Scientific Research (NWO).

¹B. Hoex, J. J. H. Gielis, M. C. M. van de Sanden, and W. M. M. Kessels, *J. Appl. Phys.* **104**, 113703 (2008).

²G. Agostinelli, A. Delabie, P. Vitanov, Z. Alexieva, H. F. W. Dekkers, S. D. Wolf, and G. Beaucarne, *Sol. Energy Mater. Sol. Cells* **90**, 3438 (2006).

³B. Hoex, S. B. S. Heil, E. Langereis, M. C. M. van de Sanden, and W. M. M. Kessels, *Appl. Phys. Lett.* **89**, 042112 (2006).

⁴B. Hoex, J. Schmidt, R. Bock, P. P. Altermatt, M. C. M. van de Sanden, and W. M. M. Kessels, *Appl. Phys. Lett.* **91**, 112107 (2007).

⁵J. J. H. Gielis, B. Hoex, M. C. M. van de Sanden, and W. M. M. Kessels, *J. Appl. Phys.* **104**, 073701 (2008).

⁶G. Dingemans, R. Seguin, P. Engelhart, M. C. M. van de Sanden, and W. M. M. Kessels, *Phys. Status Solidi (RRL)* **4**, 10 (2010).

⁷G. Dingemans, M. C. M. van de Sanden, and W. M. M. Kessels, *Electrochem. Solid-State Lett.* **13**, H76 (2010).

⁸J. J. H. Gielis, P. M. Gevers, I. M. P. Aarts, M. C. M. van de Sanden, and W. M. M. Kessels, *J. Vac. Sci. Technol. A* **26**, 1519 (2008).

⁹P. Lautenschlager, M. Garriga, L. Vina, and M. Cardona, *Phys. Rev. B* **36**, 4821 (1987).

¹⁰G. Erley, R. Butz, and W. Daum, *Phys. Rev. B* **59**, 2915 (1999).

¹¹A. Rumpel, B. Manschwetus, G. Lilienkamp, H. Schmidt, and W. Daum, *Phys. Rev. B* **74**, 081303 (2006).

¹²W. Daum, H. J. Krause, U. Reichel, and H. Ibach, *Phys. Rev. Lett.* **71**, 1234 (1993).

¹³C. Meyer, G. Lupke, U. Emmerichs, F. Wolter, H. Kurz, C. H. Bjorkman, and G. Lucovsky, *Phys. Rev. Lett.* **74**, 3001 (1995).

¹⁴G. Erley and W. Daum, *Phys. Rev. B* **58**, R1734 (1998).

¹⁵D. Hoogeland, K. B. Jinesh, F. Roozeboom, W. F. A. Besling, M. C. M. van de Sanden, and W. M. M. Kessels, *J. Appl. Phys.* **106**, 114107 (2009).

¹⁶P. Ericsson, S. Bengtsson, and J. Skarp, *Microelectron. Eng.* **36**, 91 (1997).

¹⁷J. Buckley, B. D. Salvo, D. Deleruyelle, M. Gely, G. Nicotra, S. Lombardo, J. F. Damlencourt, P. Hollinger, F. Martin, and S. Deleonibus, *Microelectron. Eng.* **80**, 210 (2005).

¹⁸J. J. H. Gielis, P. J. van den Oever, B. Hoex, M. C. M. van de Sanden, and W. M. M. Kessels, *Phys. Rev. B* **77**, 205329 (2008).

¹⁹J. J. H. Gielis, B. Hoex, P. J. van den Oever, M. C. M. van de Sanden, and W. M. M. Kessels, *Thin Solid Films* **517**, 3456 (2009).